



Contents lists available at ScienceDirect

Biochemical and Biophysical Research Communications

journal homepage: [www.elsevier.com/locate/ybbrc](http://www.elsevier.com/locate/ybbrc)

## Structural and functional insights into the Asp1/2/3 complex mediated secretion of *pneumococcal* serine-rich repeat protein PsrP

Cong Guo<sup>1</sup>, Zhang Feng<sup>1</sup>, Gang Zuo, Yong-Liang Jiang, Cong-Zhao Zhou, Yuxing Chen<sup>\*\*</sup>, Wen-Tao Hou<sup>\*</sup>

Hefei National Laboratory for Physical Sciences at the Microscale and School of Life Sciences, University of Science and Technology of China, Hefei, Anhui, 230026, China

### ARTICLE INFO

#### Article history:

Received 23 January 2020

Accepted 27 January 2020

Available online xxx

#### Keywords:

Crystal structure

Accessory sec protein

aSec system

Serine-rich-repeat protein

*Streptococcus pneumoniae*

### ABSTRACT

The accessory sec system consisting of seven conserved components is commonly distributed among pathogenic Gram-positive bacteria for the secretion of serine-rich-repeat proteins (SRRPs). Asp1/2/3 protein complex in the system is responsible for both the O-acetylation of GlcNAc and delivering SRRPs to SecA2. However, the molecular mechanism of how Asp1/2/3 transport SRRPs remains unknown. Here, we report the complex structure of Asp1/2/3 from *Streptococcus pneumoniae* at 2.9 Å. Further functional assays indicated that Asp1/2/3 can stimulate the ATPase activity of SecA2. In addition, the deletion of *asp1/2/3* gene resulted in the accumulation of a secreted version of PsrP with an altered glycoform in protoplast fraction of the mutant cell, which suggested the modification/transport coupling of the substrate. Altogether, these findings not only provide structural basis for further investigations on the transport process of SRRPs, but also uncover the indispensable role of Asp1/2/3 in the accessory sec system.

© 2020 Elsevier Inc. All rights reserved.

### 1. Introduction

*Streptococcus pneumoniae* is an important opportunistic pathogen that colonizes in the mucosal surfaces of the human upper respiratory tract [1,2], which causes otitis media, sinusitis, community-acquired pneumonia, septicemia, etc [3]. With the abuse of drugs, *S. pneumoniae* has obtained increasing resistance to multiple classes of antibiotics [4], which made it urgent to develop new anti-mycobacterial drugs. The serine rich repeat glycoproteins (SRRPs) are a large family of adhesions on the surface of certain Gram-positive bacteria which play an important role in colonization and contribute to invasive disease [5–9]. *S. pneumoniae* TIGR4 encodes a SRRP, termed PsrP (pneumococcal serine-rich repeat protein), the N-terminal region of which mediates bacterial adhering to cell surface for binding with keratin [10–12]. In addition, PsrP also promotes biofilm formation [13,14], bacterial colonization and aggression [7,15,16]. Given the importance of PsrP in

pathogenicity, the glycosylation and maturation of PsrP have been extensively studied [11,17], except for its transportation.

PsrP is specifically transported by the accessory secretory system (aSec system) [16,18]. The aSec system consists of seven proteins, two core proteins SecA2 and SecY2, and five accessory proteins Asp1–Asp5 [19]. SecA2 and SecY2 are homologs of SecA and SecY, so it is considered that the aSec system utilizes similar mechanism with the canonical Sec system in protein transportation [7,20]. SecY2 alongside with Asp4 and Asp5 forms a channel that transports PsrP out of the cytoplasm, and SecA2 provides the energy for the entire transport process by hydrolyzing ATP [19]. In *Streptococcus gordonii*, Asp3 mediates multiple protein-protein interactions within the aSec system, including Asp1, Asp2, and SecA2 [21]. This complicity of aSec interaction network was further confirmed through the identification of complex formed by Asp proteins and SecA2 in *Streptococcus parasanguinis* [22]. In many Gram-positive bacteria, deletion of *asp1/2/3* could block the transport of SRRPs, indicating a crucial role of Asp1/2/3 in aSec system [21,23–25]. In a recently published paper, Asp2 was found to be able to mediate the O-acetylation of GlcNAc residues on GspB in *S. gordonii* [5,20]. Despite many efforts have been made to explore the mechanism of how SRRPs can be transported cross the cell membrane, little is known about the exact role of Asp1/2/3 for PsrP

\* Corresponding author.

\*\* Corresponding author.

E-mail addresses: [cyxing@ustc.edu.cn](mailto:cyxing@ustc.edu.cn) (Y. Chen), [todvince@mail.ustc.edu.cn](mailto:todvince@mail.ustc.edu.cn) (W.-T. Hou).

<sup>1</sup> These authors contribute equally to this work.

transport through aSec system in *S. pneumoniae*.

Here, we show the crystal structure of Asp1/2/3 complex from *S. pneumoniae* at 2.9 Å. Structural analysis combined with multi-sequence alignment showed that inter-molecule interactions are conserved among Asp1/2/3 complex homologs. Results of functional studies suggested that Asp1/2/3 could promote substrate translocation by stimulating the ATPase activity of SecA2. Moreover, altered glycosylation of secreted PsrP in *asp1/2/3* deletion mutant uncovered the role of Asp1/2/3 in coupling the glycosylation and transportation of PsrP. These findings provide structural and functional insights into the Asp1/2/3 complex mediated secretion of PsrP.

## 2. Material and method

### 2.1. Construction, expression and purification of Asp1/2/3 and SecA2

We cloned *S. pneumoniae* TIGR4 *asp1/2/3* into a modified pET28a vector with a C-terminal 6 × His-tag on Asp3. The plasmid was transformed into BL21 (DE3). Cells were grown in LB culture medium (10 g of tryptone, 5 g of yeast extract and 10 g of NaCl per liter) containing 30 μg mL<sup>-1</sup> kanamycin at 37 °C. When OD<sub>600</sub> reached 0.6–0.8, the cells were induced with 0.2 mM isopropyl β-D-1-thiogalactopyranoside (IPTG) at 25 °C for 16 h. Then cells were harvested by centrifugation and resuspended in the lysis buffer (25 mM Tris-HCl 8.0, 100 mM NaCl). After sonification and centrifugation, the supernatant was pooled and loaded onto a Ni-NTA column pre-equilibrated with the binding buffer (25 mM Tris-HCl 8.0, 100 mM NaCl). The target protein Asp1/2/3 complex was eluted with 400 mM imidazole and then applied to a Superdex 200 column (10/300 GL, GE Healthcare) pre-equilibrated with the binding buffer.

*S. pneumoniae* TIGR4 *secA2* was cloned into a modified pET30a vector (V28E5) [26] with N-terminal MBP-tag. The plasmid was transformed into BL21 (DE3). When OD<sub>600</sub> reached 0.6–0.8, the cells were induced with 0.2 mM IPTG at 16 °C for 20 h. Then cells were harvested by centrifugation and resuspended in lysis buffer (25 mM Tris-HCl 8.0, 100 mM NaCl and 5% glycerol). After sonification and centrifugation, the supernatant was pooled and loaded onto a MBP column pre-equilibrated with the binding buffer (25 mM Tris-HCl 8.0, 100 mM NaCl and 5% glycerol). The target protein SecA2 complex was eluted with 10 mM maltose and then applied to a Superdex 200 column (10/300 GL, GE Healthcare) pre-equilibrated with the binding buffer.

### 2.2. Crystallization, data collection, and structure determination

Crystallization of native Asp1/2/3 complex was performed by the hanging-drop vapor-diffusion method at 293 K. The native Asp1/2/3 crystals were obtained against the reservoir solution of 0.1 M Tris 8.0, 15% PEG 6000. All the crystals were transferred to the cryoprotectant (reservoir solution supplemented with 25% sucrose) and flash-cooled in liquid nitrogen. X-ray diffraction data were collected at 100 K in a liquid nitrogen stream, using beamline BL17U [27] at the Shanghai Synchrotron Radiation Facility (SSRF) of China at the wavelength of 0.97915 Å. All diffraction data were integrated and scaled with *HKL2000* [28].

The structure of complex Asp1/2/3 was determined by molecular replacement with MOLREP [29]. The search model using for structure analysis was the structure of *S. gordonii* Asp1/3 (PDB entry 5vae) [7]. The initial model was further refined by the maximum likelihood method implemented in *Refmac5* [26] as part of the CCP4i program suite [27], and rebuilt interactively using the program *Coot* [28]. The final model was evaluated with the web service

**Table 1**

Crystal parameters, data collection, and structure refinement.

	Asp1/2/3
<b>Data collection</b>	
Wavelength (Å)	0.97915
Space group	P3 <sub>1</sub> 21
<b>Unit cell parameters</b>	
<i>a</i> , <i>b</i> , <i>c</i> (Å)	101.158, 101.158, 196.851
$\alpha$ , $\beta$ , $\gamma$ (°)	90.00, 90.00, 120.00
Resolution range (Å) <sup>a</sup>	50.0–2.90 (3.00–2.90)
Unique reflections	26,531 (2586)
Completeness (%)	99.8 (100.0)
$\langle I/\sigma(I) \rangle$	12.2 (3.6)
$R_{\text{merge}}^b$ (%)	13.6 (52.3)
Average redundancy	4.7 (4.9)
<b>Structure refinement</b>	
Resolution range (Å)	42.94–2.90
$R_{\text{factor}}^c/R_{\text{free}}^d$ (%)	19.7 (24.2)
Number of protein atoms	6497
Number of water atoms	90
RMSD <sup>e</sup> bond lengths (Å)	0.01
RMSD bond angles (°)	1.30
Mean B factors (Å <sup>2</sup> )	32.37
<b>Ramachandran plot (residues, %)<sup>f</sup></b>	
Most favored (%)	96.31
Additional allowed (%)	3.69
Protein Data Bank entry	6LNW

<sup>a</sup> The values in parentheses refer to statistics in the highest bin.

<sup>b</sup>  $R_{\text{merge}} = \frac{\sum_{hkl} \sum_i |I_i(hkl) - \langle I(hkl) \rangle|}{\sum_{hkl} \sum_i I_i(hkl)}$ , where  $I_i(hkl)$  is the intensity of an observation, and  $\langle I(hkl) \rangle$  is the mean value for its unique reflection. Summations are over all reflections.

<sup>c</sup>  $R_{\text{factor}} = \frac{\sum_h |F_o(h) - F_c(h)|}{\sum_h F_o(h)}$ , where  $F_o$  and  $F_c$  are the observed and calculated structure-factor amplitudes, respectively.

<sup>d</sup>  $R_{\text{free}}$  was calculated with 5% of the data excluded from the refinement.

<sup>e</sup> RMSD from ideal values.

<sup>f</sup> Categories were defined by MolProbity.

*Molprobity* [29]. Crystallographic parameters were listed in Table 1. All structure figures were prepared with PyMOL (<http://www.pymol.org>).

### 2.3. Acetyltransferase activity assays

The acetyltransferase activity of Asp1/2/3 was assayed by high performance liquid chromatography (HPLC). The assays were performed at 25 °C for 30 min in a final volume of 20 μL containing 50 mM Sodium phosphate 7.4, 1.28 μM Asp1/2/3, and different concentrations of p-nitrophenyl acetate (pNP-Ac) (dissolved in ethanol) as the acetyl donor. The reactions were initiated by adding pNP-Ac and terminated by adding 10% Trichloroacetic acid (TCA). The samples were centrifuged at 12,000 ×g for 10 min, and 10 μL of supernatant was applied to the HPLC system (Agilent 1200 Series). The buffer of 50 mM sodium citrate, pH 6.0 with 40% acetonitrile, was used as the mobile phase to equilibrate the column (Eclipse XDB-C18 column, Agilent). The product pNP was monitored by the absorption at 290 nm and was assigned based on the retention time of the standards. Three independent assays were performed to calculate the means and standard deviations for  $K_m$  value.

### 2.4. ATPase activity assays

The SecA2 used for the ATPase activity assay was purified as mentioned above. The reaction mixtures were in a final volume of 100 μL containing 50 mM Tris-HCl, pH 8.0, 150 mM KCl, 2 mM MgCl<sub>2</sub> and ATP at varying concentrations. For each reaction sample, 0.5 μM of SecA2 was added. Then the reactions were carried out at 37 °C for 50 min and the amount of released Pi was quantitatively measured using the Malachite green in 96-well plates. The mixture was incubated for 30 min at 4 °C before the activity was measured

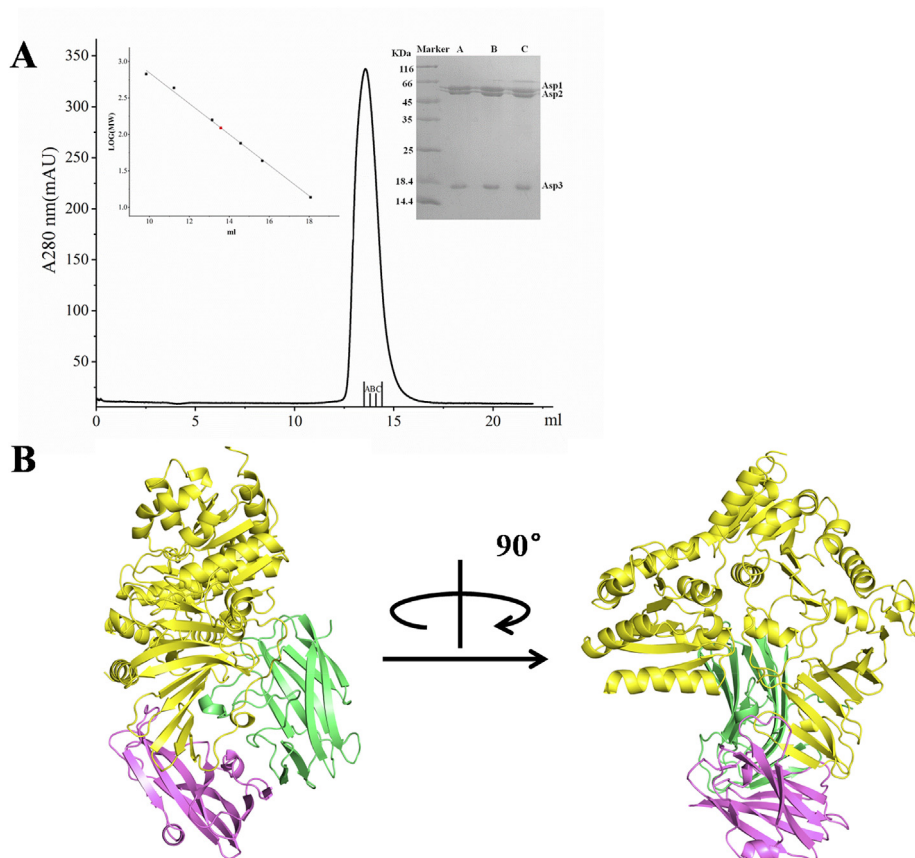


**Fig. 1.** Overall structure of Asp1/2/3. (A) Gel filtration chromatography of the Asp1/2/3 complex and Coomassie blue-stained SDS gel electrophoresis of corresponding peak fractions from gel filtration chromatography. (B) Cartoon representation of Asp1/2/3. Asp1, Asp2 and Asp3 are colored in yellow, purple and green, respectively. (For interpretation of the references to color in this figure legend, the reader is referred to the Web version of this article.)

by monitoring the increase of absorbance at 630 nm. Three independent assays were performed. In addition, we added 10  $\mu$ M Asp1/2/3 into the reaction system, and use the same method to measure the ATPase activity of SecA2. All the measurements were done in triplicate.

#### 2.5. Secretion and glycosylation assay of PsrP

The *asp1/2/3* deletion mutant of *S. pneumoniae* was generated from the strain TIGR4 by allelic replacement as described previously [30]. In brief, the upstream region of *asp1* and downstream regions of *asp3* in strain TIGR4 were separately amplified from genomic DNA by PCR. The kanamycin-resistant Janus cassette fragment was amplified from the prepared genomic DNA of *S. pneumoniae* strain ST588 [31]. These fragments were integrated by overlapping PCR. Purified PCR products were then transformed into the strain TIGR4 to select kanamycin-resistant colonies on blood agar plates. The replacement of the whole *asp1/2/3* coding region with the Janus cassette was selected by kanamycin and was then detected and confirmed by PCR and DNA sequencing.

We cloned *psrP1-633* with a N-terminal flag-tag into a Zn<sup>2+</sup> inducible pJWV25 plasmid [32]. These plasmids were transformed into the wild type and *asp1/2/3* deletion strain, and the strain was grown in THY culture medium (30 g of Todd-Hewitt Broth and 5 g of yeast extract per liter) containing 0.15 mM ZnCl<sub>2</sub>. Then the cultures were fractionated into the culture medium and cell pellet by centrifugation. A total of 20  $\mu$ L of the culture media or protoplast was mixed with loading buffer and then resolved by SDS-PAGE. Western blotting with anti-FLAG antibody was carried out for the

detection of PsrP variants.

### 3. Results

#### 3.1. Overall structure of Asp1/2/3

It was reported that Asp1/2/3 may function as a complex [5,7]. However, the exact stoichiometry of the three proteins is still unknown. To study the structure and function of the Asp1/2/3 of *S. pneumoniae*, we overexpressed Asp1/2/3 in *E. coli*. The purification profile indicated that the output of the Asp1/2/3 proteins gave a single peak of ~124.8 kDa (Fig. 1A), which is approximately identical with the sum of the theoretical molecular mass of three Asp proteins. The equal molar ratio of Asp1/2/3 was further affirmed by estimating the intensity of stained bands in the subsequent gel electrophoresis (Fig. 1A). Together, these results enabled us to confirm that Asp1/2/3 form a stable complex with a stoichiometry of 1:1:1.

Given a high sequence similarity of Asps in *S. pneumoniae* and *S. gordonii*, we determined the crystal structures of Asp1/2/3 complex from *S. pneumoniae* at 2.9 Å (PDB entry 6lnw) in the space group P3<sub>1</sub>21 by molecular replacement using Asp1/3 from *S. gordonii* (SgAsp1/3; PDB entry 5vae) (Fig. 1B). Structural similarity analysis also showed that Asp1 and Asp3 have the high structural homology with SgAsp1 and SgAsp3, and superpositions yielded RMSDs of 1.26 and 1.27 Å over 476 and 130 C $\alpha$  atoms, respectively. In our structure, Asp1 molecule contains residues Met1-Lys524, and a segment covering residues Asn380-Arg408 cannot be modeled due to the poor electron density. Asp3 molecule contains

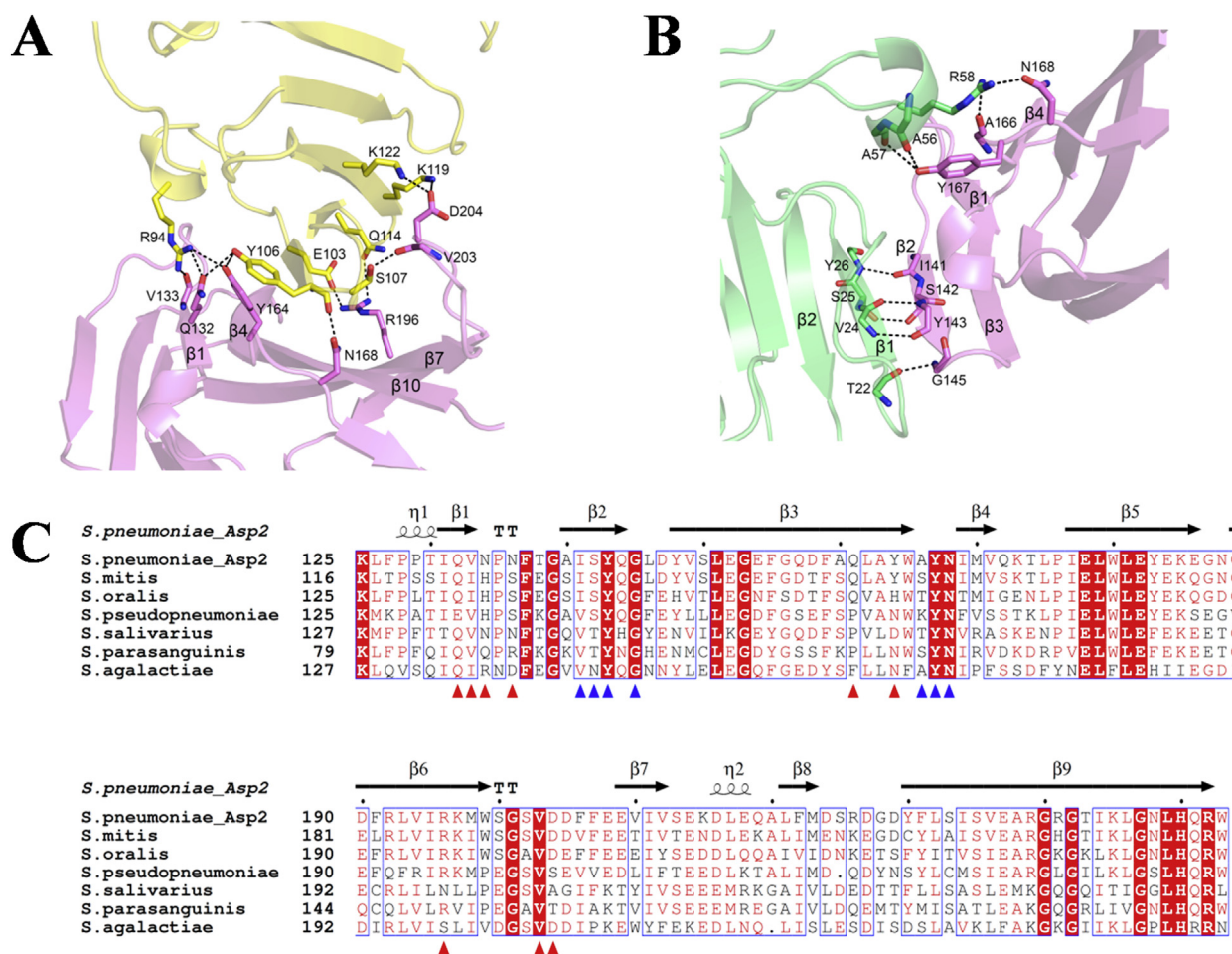


**Fig. 2.** Structure analysis of Asp1/2/3. (A) Interactions between Asp2 and Asp1. The interacting residues are shown as sticks. (B) Interactions between Asp2 and Asp3. The interacting residues are shown as sticks. (C) Multiple-sequence alignment of *S. pneumoniae* Asp2 and its homologs. Conserved residues in Asp2 and Asp3 marked with red and blue triangles, respectively. The alignment was performed with the programs Multalin and Esript. The secondary structural elements of Asp2 are shown above the sequences. (For interpretation of the references to color in this figure legend, the reader is referred to the Web version of this article.)

Ile2-Arg144. The full-length Asp2 was applied for crystallization, but only the segment of residues Lys125-Trp253 could be traced in the electron density map, suggesting Asp2 degraded during crystallization. In our structure, each asymmetric unit contains one molecule of Asp1/2/3, which confirms the ratio of the complex. Asp1 has two Rossmann-like folds and an extended  $\beta$ -sheet domain (EBD), forming a U-shaped structure like GtfA and GtfB [7], whereas Asp2 and Asp3 share a similar jelly-roll fold with each consisting of two layers of anti-parallel  $\beta$  sheets.

### 3.2. Interaction interface of Asp1/2/3

Interface analysis using PBDDePISA [33] indicated that the largest interface with a buried area of 1695  $\text{\AA}^2$  is formed by Asp1 and Asp3. The stabilization is mainly achieved by hydrogen bonds and salt bridges, which are formed by residues located at the tips of the  $\beta$ -strands of Asp3 and EBD of Asp1, along with the cleft between two Rossmann-like folds, as analyzed in homologous structure of SgAsp1/3 [7]. In addition, Asp2 further stabilized the Asp1/2/3 complex by directly interacting with both Asp1 and Asp3, resulting in buried areas of 760  $\text{\AA}^2$  and 523  $\text{\AA}^2$ , respectively. In the complex structure of Asp1/2/3, the EBD domain of Asp1 adopts a vertical orientation relative to Asp3. The N-terminal  $\beta$ -strands of the EBD domain of Asp1 is embedded in the groove formed by strands  $\beta$ 1,  $\beta$ 4,  $\beta$ 7 and

$\beta$ 10 of Asp2 (Fig. 2A). Hydrogen bonds including Tyr106-Gln132, Arg94-Gln132, Arg94-Val133 and Cys102-Asn134, in addition to a couple of salt bridges Glu103-Arg196, Lys119-Asp204 and Lys122-Asp204 contribute to the interaction between Asp1 and Asp2. Structural analysis showed that Asp2 and Asp3 form a continuous extended  $\beta$  sheet via edge-to-edge interaction between the strands  $\beta$ 1 of Asp2 and  $\beta$ 2 of Asp3 (Fig. 2B). In addition, a short helix between  $\beta$ 3 and  $\beta$ 4 of Asp2 projects towards Asp3 to interact with the loop $\beta$ 4- $\beta$ 5 by hydrogen bonds of Ala166-Arg58, Tyr167-Ala56, Tyr167-Ala57 and Asn168-Arg58, further stabilizes the interaction between Asp2 and Asp3. Structure-based multiple-sequence alignment showed that these residues at interaction interface of Asp2 are highly conserved in *S. pneumoniae* and its homologs (Fig. 2C), suggesting the necessity of the formation of Asp1/2/3 complex for full function.

### 3.3. Biochemical characterization of Asp1/2/3

Previous reports showed that SgAsp3 can interact with SecA2 using a direct yeast two-hybrid assay [21], and the interaction may promote the export of GspB in *S. gordonii*. However, detailed molecular mechanism underlying the participation of Asp1/2/3 into the process of substrate transport is poorly understood. We performed ATPase assays to find out whether Asp1/2/3 could affect the

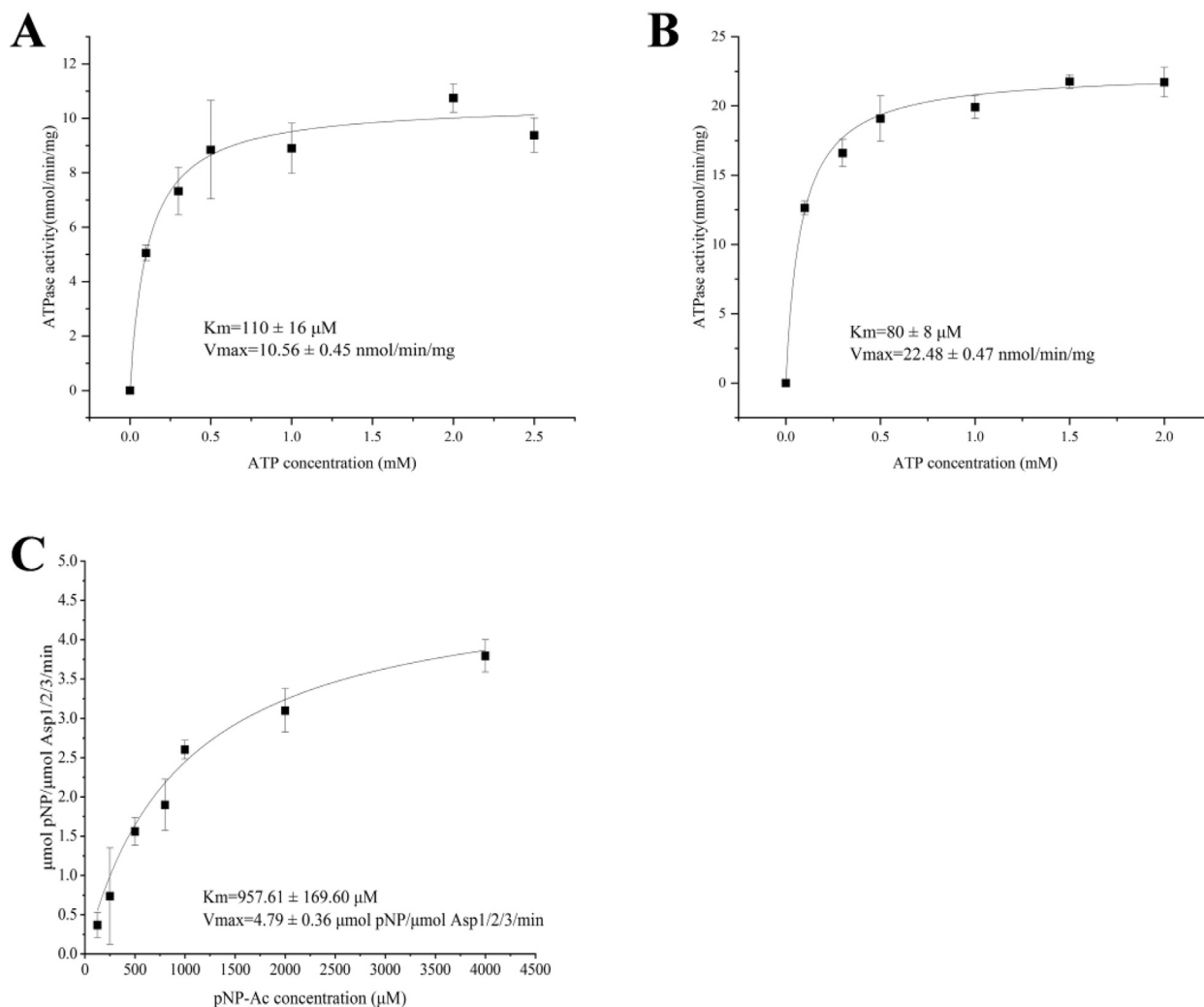


**Fig. 3.** Biochemical characterization of Asp1/2/3. ATP at various concentrations was incubated with 0.5  $\mu\text{M}$  SecA2 in the (A) absence or (B) presence of Asp1/2/3. Velocities were obtained from the slopes of the ADP accumulation curves and fitted to the Michaelis-Menten model with a  $V_{\text{max}}$  of  $10.56 \pm 0.45$  and  $22.48 \pm 0.47$  nmol ATP/min/mg SecA2, and a  $K_m$  of  $110 \pm 16$  and  $80 \pm 8$   $\mu\text{M}$ , respectively. (C) Determination of acetyltransferase activity of Asp1/2/3 complex.

ATPase activity of SecA2. We determined the enzymatic parameters of SecA2 in the presence or absence of Asp1/2/3. Calculations of enzymatic parameters gave a  $K_m$  of  $110 \pm 16$   $\mu\text{M}$  and a  $V_{\text{max}}$  of  $10.56 \pm 0.45$  nM ATP/min/mg protein in the absence of Asp1/2/3 (Fig. 3A). In contrast, the addition of Asp1/2/3 resulted in a decreased  $K_m$  of  $80 \pm 8$   $\mu\text{M}$  and increased  $V_{\text{max}}$  of  $22.48 \pm 0.47$  nM ATP/min/mg protein (Fig. 3B). These results suggested that Asp1/2/3 can stimulate the ATPase activity of SecA2, and could principally accelerate substrates to pass through aSec system.

Despite the previous report proved that Asp2 mediates the O-acetylation of GlcNAc residues on GspB in vitro, whether Asp1 and Asp3 would affect the activity of Asp2 is under estimation. To explore the acetyltransferase activity of Asp2 in presence of Asp1 and Asp3, we performed the hydrolysis activity assay with p-nitrophenyl acetate (pNP-Ac) as the acetyl donor and further determined the enzymatic parameters of Asp1/2/3 (Fig. 3C). Calculations of enzymatic parameters gave a  $K_m$  of  $957.16 \pm 169.60$   $\mu\text{M}$  and a  $V_{\text{max}}$  of  $4.79 \pm 0.36$   $\mu\text{M pNP}/\text{min}/\mu\text{M Asp1/2/3}$  which is comparable to that of Asp2 in the previous report. Thus, the Asp1 and Asp3 have no significant effect on acetyltransferase activity of Asp2.

### 3.4. Asp1/2/3 is required for the secretion and glycosylation of PsrP

To further explore whether Asp1/2/3 affects the transport of PsrP, we constructed a mutant *S. pneumoniae* with the deletion of gene *asp1/2/3*. This mutant strain was used to assess the secretion of gene *psrP633flag*, a truncated version of PsrP lacking the cell wall-anchoring LPxTG motif (Fig. 4A). As shown in Fig. 4B, the slightly smeared bands of PsrP633flag, mostly due to the relatively complicated and heterogeneous glycosylation in *S. pneumoniae* [11], was detected only in the culture media (Lane 3). However, the detection of the PsrP633flag in mutant showing a clear band in the protoplast fraction (Lane 2) rather than the media (Lane 1) suggested the failure of PsrP633flag export. In addition, the deletion of *asp1/2/3* resulted in PsrP633flag with altered electrophoretic mobility, suggesting that Asp1/2/3 can affect the glycosylation of PsrP. Altogether, these results showed that Asp1/2/3 is not only required for the secretion but also the correct glycosylation of PsrP.

## 4. Discussion

Accessory sec protein Asp1/2/3 is conserved among pathogen

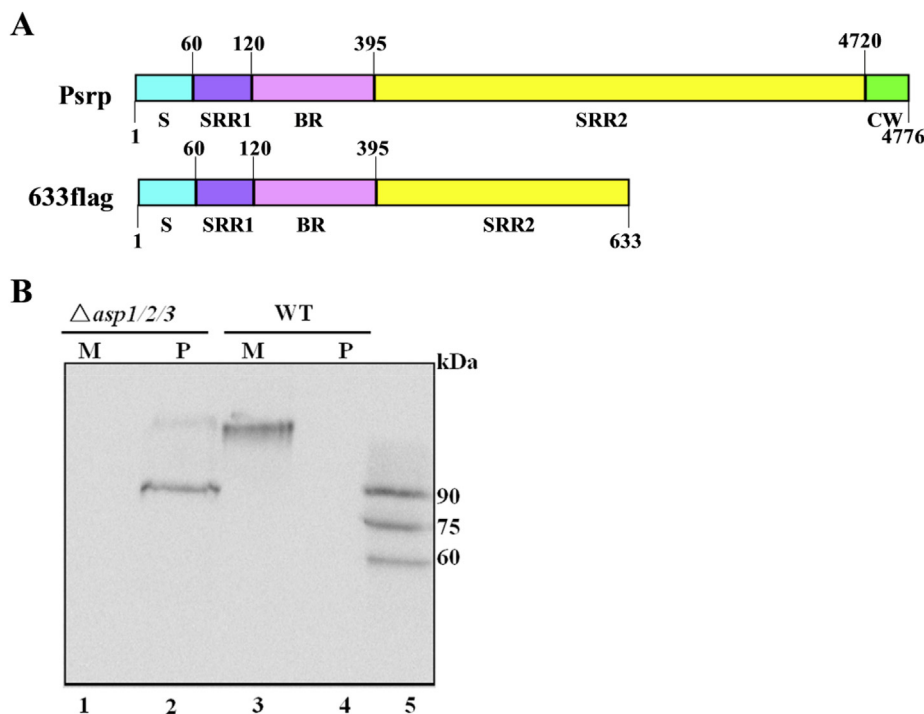


**Fig. 4.** Asp1/2/3 affects PsrP transport and glycosylation. (A) Domain organization of wild-type PsrP and PsrP633flag. PsrP is organized into five domains: the N-terminal signal sequence (S) for extracellular translocation of PsrP, two putatively glycosylated serine rich repeat regions (SRR1 and SRR2), the binding region (BR) domain and the cell wall domain (CW). (B) Western blotting of media and protoplast of *S. pneumoniae* and its *asp1/2/3* mutant.

bacteria secreting SRRPs. Asp1/2/3 in *S. gordonii* has been studied considerably and has been shown to be essential for substrate export. Recent reports showed that the Asp2 alters the glycosylation pattern of GspB by acetylating the GlcNAc residues. In addition, failing of GspB export abolished the acetylation of GspB, indicating a coupled mechanism for the modification and transport of adhesins. However, little is known on the role of Asp1/2/3 complex in transport of *S. pneumoniae* glycoprotein PsrP.

Here, we solved the structure of Asp1/2/3 from *S. pneumoniae* at 2.9 Å. Structural analysis combined with multi-sequence alignment showed conserved interaction interfaces in Asp1/2/3 and homologs, which advances our understanding on the formation of Asp1/2/3 complex. Moreover, the functional assays showed that Asp1/2/3 not only stimulate the ATPase activity of SecA2 but affect the export and glycosylation of PsrP, suggesting Asp1/2/3 an indispensable role for the maturation of glycosylated PsrP.

Altogether, these results enable us to illustrate different roles of three accessory sec proteins. In Asp1/2/3 protein complex, Asp2 plays a core role to acetylate the GlcNAc residues. Asp1 functions as a carbohydrate-binding protein like GtfB, meanwhile Asp2 strengthens the interaction between Asp1 and Asp3 to further stabilize the complex. The stimulation of the ATPase activity of SecA2 initially uncovers the regulation functions of Asp1/2/3. However, more structural and biochemical investigations are needed to clearly elucidate the roles of Asp1/2/3 protein complex in the transport process of SRRPs.

## Funding

This work is supported by the National Natural Science Foundation of China (Grants No.31770787 and No. 31670732).

## Declaration of competing interest

These authors declare no conflicts of interest.

## Acknowledgements

We thank the staff at the Shanghai Synchrotron Radiation Facility for technical assistance.

## References

- [1] B. Henriques-Normark, E.I. Tuomanen, The pneumococcus: epidemiology, microbiology, and pathogenesis, *Cold Spring Harb. Perspect. Med.* 3 (2013).
- [2] J.N. Weiser, D.M. Ferreira, J.C. Paton, *Streptococcus pneumoniae*: transmission, colonization and invasion, *Nat. Rev. Microbiol.* 16 (2018) 355–367.
- [3] L.E. Keller, D.A. Robinson, L.S. McDaniel, Nonencapsulated *Streptococcus pneumoniae*: emergence and pathogenesis, *mBio* 7 (2016), e01792.
- [4] M. Regine Cherazard, M. Epstein, T.-L. Doan, M. Tanzila Salim, S. Bharti, M.A. Smith, Antimicrobial resistant *Streptococcus pneumoniae*: prevalence, mechanisms, and clinical implications, *Am. J. Therapeut.* 24 (3) (2017).
- [5] R. Seepersaud, D. Sychantha, B.A. Bensing, A.J. Clarke, P.M. Sullam, O-acetylation of the serine-rich repeat glycoprotein GspB is coordinated with accessory Sec transport, *PLoS Pathog.* 13 (2017), e1006558.
- [6] K.A. Kline, S. Falker, S. Dahlberg, S. Normark, B. Henriques-Normark, Bacterial adhesins in host-microbe interactions, *Cell Host Microbe* 5 (2009) 580–592.
- [7] Y. Chen, B.A. Bensing, R. Seepersaud, W. Mi, M. Liao, P.D. Jeffrey, A. Shajahan, R.N. Sonon, P. Azadi, P.M. Sullam, T.A. Rapoport, Unraveling the sequence of cytosolic reactions in the export of GspB adhesin from *Streptococcus gordonii*, *J. Biol. Chem.* 293 (2018) 5360–5373.
- [8] M. Zhou, H. Wu, Glycosylation and biogenesis of a family of serine-rich bacterial adhesins, *Microbiology* 155 (2009) 317–327.
- [9] A. Lizcano, C.J. Sanchez, C.J. Orihuela, A role for glycosylated serine-rich repeat proteins in gram-positive bacterial pathogenesis, *Mol. Oral. Microbiol.* 27 (2012) 257–269.
- [10] P. Shivshankar, C. Sanchez, L.F. Rose, C.J. Orihuela, The *Streptococcus pneumoniae* adhesin PsrP binds to Keratin 10 on lung cells, *Mol. Microbiol.* 73 (2009) 663–679.
- [11] Y.L. Jiang, H. Jin, H.B. Yang, R.L. Zhao, S. Wang, Y. Chen, C.Z. Zhou, Defining the enzymatic pathway for polymorphic O-glycosylation of the pneumococcal serine-rich repeat protein PsrP, *J. Biol. Chem.* 292 (2017) 6213–6224.
- [12] M. Bandara, J.M. Skehel, A. Kadioglu, I. Collinson, A.H. Nobbs, A.J. Blocker, H.F. Jenkinson, The accessory Sec system (SecY2A2) in *Streptococcus pneumoniae* is involved in export of pneumolysin toxin, adhesion and biofilm formation, *Microb. Infect.* 19 (2017) 402–412.
- [13] N.M. van Sorge, D. Quach, M.A. Gurney, P.M. Sullam, V. Nizet, K.S. Doran, The group B streptococcal serine-rich repeat 1 glycoprotein mediates penetration of the blood-brain barrier, *J. Infect. Dis.* 199 (2009) 1479–1487.
- [14] E.H. Froeliger, P. Fives-Taylor, *Streptococcus parasanguis* fimbria-associated

- adhesin fap1 is required for biofilm formation, *Infect. Immun.* 69 (2001) 2512–2519.
- [15] P.S. Handley, F.F. Correia, K. Russell, B. Rosan, J.M. DiRienzo, Association of a novel high molecular weight, serine-rich protein (SrpA) with fibril-mediated adhesion of the oral biofilm bacterium *Streptococcus cristatus*, *Oral Microbiol. Immunol.* 20 (2005) 131–140.
- [16] T. Schulte, C. Mikaelsson, A. Beaussart, A. Kikhney, M. Deshmukh, S. Wolniak, A. Pathak, C. Ebel, J. Lofling, F. Fogolari, B. Henriques-Normark, Y.F. Dufrene, D. Svergun, P.A. Nygren, A. Achour, The BR domain of PsrP interacts with extracellular DNA to promote bacterial aggregation; structural insights into pneumococcal biofilm formation, *Sci. Rep.* 6 (2016) 32371.
- [17] W.W. Shi, Y.L. Jiang, F. Zhu, Y.H. Yang, Q.Y. Shao, H.B. Yang, Y.M. Ren, H. Wu, Y. Chen, C.Z. Zhou, Structure of a novel O-linked N-acetyl-D-glucosamine (O-GlcNAc) transferase, GtfA, reveals insights into the glycosylation of pneumococcal serine-rich repeat adhesins, *J. Biol. Chem.* 289 (2014) 20898–20907.
- [18] M.E. Feltcher, M. Braunstein, Emerging themes in SecA2-mediated protein export, *Nat. Rev. Microbiol.* 10 (2012) 779–789.
- [19] M. Bandara, R.A. Corey, R. Martin, J.M. Skehel, A.J. Blocker, H.F. Jenkinson, I. Collinson, Composition and activity of the non-canonical gram-positive SecY2 complex, *J. Biol. Chem.* 291 (2016) 21474–21484.
- [20] R. Seepersaud, B.A. Bensing, Y.T. Yen, P.M. Sullam, The accessory Sec protein Asp2 modulates GlcNAc deposition onto the serine-rich repeat glycoprotein GspB, *J. Bacteriol.* 194 (2012) 5564–5575.
- [21] B.A.B. Ravin Seepersaud, Yihfen T. Yen, Paul M. Sullam, Asp3 mediates multiple protein–protein interactions within the accessory Sec system of *Streptococcus gordonii*, *Mol. Microbiol.* 78 (2010) 490–505.
- [22] M. Zhou, H. Zhang, F. Zhu, H. Wu, Canonical SecA associates with an accessory secretory protein complex involved in biogenesis of a streptococcal serine-rich repeat glycoprotein, *J. Bacteriol.* 193 (2011) 6560–6566.
- [23] D. Takamatsu, B.A. Bensing, P.M. Sullam, Genes in the accessory sec locus of *Streptococcus gordonii* have three functionally distinct effects on the expression of the platelet-binding protein GspB, *Mol. Microbiol.* 52 (2004) 189–203.
- [24] H. Echlin, F. Zhu, Y. Li, Z. Peng, T. Ruiz, G.J. Bedwell, P.E. Prevelige Jr., H. Wu, Gap2 promotes the formation of a stable protein complex required for mature Fap1 biogenesis, *J. Bacteriol.* 195 (2013) 2166–2176.
- [25] Y. Li, Y. Chen, X. Huang, M. Zhou, R. Wu, S. Dong, D.G. Pritchard, P. Fives-Taylor, H. Wu, A conserved domain of previously unknown function in Gap1 mediates protein–protein interaction and is required for biogenesis of a serine-rich streptococcal adhesin, *Mol. Microbiol.* 70 (2008) 1094–1104.
- [26] T. Jin, W. Chuenchor, J. Jiang, J. Cheng, Y. Li, K. Fang, M. Huang, P. Smith, T.S. Xiao, Design of an expression system to enhance MBP-mediated crystallization, *Sci. Rep.* 7 (2017) 40991.
- [27] Y.F. Wang Qi Sheng, The macromolecular crystallography beamline of SSRF, *Nucl. Sci. Tech.* 26 (2015) 5.
- [28] W.M. Zbyszek Otwinowski, Processing of X-ray diffraction data collected in oscillation mode, *Methods Enzymol.* 276 (1997) 307–326.
- [29] M.D. Winn, C.C. Ballard, K.D. Cowtan, E.J. Dodson, P. Emsley, P.R. Evans, R.M. Keegan, E.B. Krissinel, A.G. Leslie, A. McCoy, S.J. McNicholas, G.N. Murshudov, N.S. Pannu, E.A. Potterton, H.R. Powell, R.J. Read, A. Vagin, K.S. Wilson, Overview of the CCP4 suite and current developments, *Acta Crystallogr. D Biol. Crystallogr.* 67 (2011) 235–242.
- [30] C.K. Sung, H. Li, J.P. Claverys, D.A. Morrison, An rpsL cassette, janus, for gene replacement through negative selection in *Streptococcus pneumoniae*, *Appl. Environ. Microbiol.* 67 (2001) 5190–5196.
- [31] L. Lu, Y. Ma, J.R. Zhang, *Streptococcus pneumoniae* recruits complement factor H through the amino terminus of CbpA, *J. Biol. Chem.* 281 (2006) 15464–15474.
- [32] A. Eberhardt, L.J. Wu, J. Errington, W. Vollmer, J.W. Veening, Cellular localization of choline-utilization proteins in *Streptococcus pneumoniae* using novel fluorescent reporter systems, *Mol. Microbiol.* 74 (2009) 395–408.
- [33] E. Krissinel, K. Henrick, Inference of macromolecular assemblies from crystalline state, *J. Mol. Biol.* 372 (2007) 774–797.